

Sensitive SERS Characterization and Analysis of Chlorpyrifos and Aldicarb Residues in Animal Feed using Gold Nanoparticles

Kyung-Min Lee^{a,*}, Danielle Yarbough^b, Mena M. Kozman^c, Timothy J. Herrman^a, Jinhyuk Park^d, Rui Wang^e, Dmitry Kurouski^e

^aOffice of the Texas State Chemist, Texas A&M AgriLife Research, Texas A&M University System, College Station, TX

^bDepartment of Chemical Engineering, Texas A&M University, College Station, TX

^cDepartment of Biology, Texas A&M University, College Station, TX

^dDepartment of Biological and Agricultural Engineering, Texas A&M University, College Station, TX

^eDepartment of Biochemistry and Biophysics, Texas A&M University, College Station, TX

Abstract

The spectroscopic method based on surface-enhanced Raman spectroscopy (SERS) technique combined with chemometric methods was developed for simple, cost-effective, and efficient analysis of chlorpyrifos (CPF) and aldicarb (ALD) pesticide residues in animal feed. Animal feeds free from the pesticides were spiked at different concentrations of CPF (0–20 mg/kg) and aldicarb (0–100 µg/kg). Gold nanoparticles were mixed with sample extract for SERS measurement. A significant spectral difference induced by the presence and different level of CPF and ALD concentration in animal feed was observed between the pesticide spiking groups. Different chemometric models applied on training datasets showed excellent classification rates (100 percent) while the models on external validation dataset exhibited lower correct classification rates (50.0–76.7 percent) with no false-negative error. The selected chemometric models for CPF and ALD quantification also showed a high predictive ability and performance. The developed models displayed no statistical significant difference between model predicted and reference values in the external validation dataset ($p < 0.01$). The study results indicate that the SERS spectroscopic method could be an effective and efficient analytical tool for pesticide analysis in highly complex animal feed matrices for screening at a point of sampling to improve food and feed safety.

Keywords: surface-enhanced Raman spectroscopy (SERS), nanoparticle, pesticide, chlorpyrifos, aldicarb, animal feed, feed safety

1. Introduction

Raman spectroscopy based on inelastic scattering of light interacting with molecular vibrations has multiplexing capabilities due to its ability to provide plenty of structural and quantitative information of molecules through high resolution and distinguishable Raman bands [42]. The Raman scattering technique depends on a polarizability of chemical bonds, particularly non-polar functional groups, and can offer well-resolved and fewer overlapped bands in aqueous environments. However, conventional Raman spectroscopy suffers from a lack of sensitivity resulting from a low efficiency of Raman scattering effect.

Surface-enhanced Raman spectroscopy (SERS) is a promising Raman technique to enhance such weak inelastic Raman scattering by using metallic nanoparticles and surface plasmon resonance effects of the substrate [7, 50]. The enhancement level and acceptance of SERS are largely determined

by its preparation method. The preparation methods reported in previous studies include chemical reduction of metallic ions, thermal decomposition, and electric/physical dispersion of nanoparticles, resulting in various nanostructures with a wide range of particle sizes [45, 14]. The designed SERS substrates can provide considerably greater sensitivity, with an enhancement factor as high as $>10^{10}$, enough to detect and identify a single molecule [53, 35]. The Raman enhancement is believed to be a local phenomenon depending on the morphology of SERS and a limited number of Raman active particles forming hot spots [26, 54]. The Raman enhancement effect has been explained by electromagnetic (EM) and charge transfer mechanisms between absorbed molecules and SERS nanoparticles, which aid an enhancement of the electromagnetic field, producing strong Raman signal [7, 37]. However, it still seems to be a challenge to understand and control optimal conditions to yield a more efficient SERS substrate, as well as to systematically develop a SERS substrate technology on the basis of well-engineered processes. In addition, in order to use the SERS technique for a routine field screening, it would be desirable

*Corresponding author: Kyung-Min Lee, Email: kml@otsc.tamu.edu, Phone: 979-458-7809, Fax: 979-845-1389

to need less expensive materials and non-hazardous chemicals, employ simpler statistical techniques, and minimize instability and morphological variations of the SERS substrates [17, 46].

Chemometrics is an interdisciplinary field that employs multivariate statistical techniques, mathematical procedures, and information technologies, to facilitate spectral data processing and interpretation to relate acquired spectra of vibrational spectroscopy to chemical reference values or process parameters [8, 40]. Chemometric algorithms have been widely used in Raman spectroscopic studies to greatly simplify and better understand a complex structure of large spectral datasets, which facilitate the generation and testing of a hypothesis and extract hidden and meaningful information from collected spectral data [9, 20]. Chemometric methods can be commonly categorized into four groups: 1) data processing (e.g., baseline correction, normalization, derivatives, deconvolution, and multiplicative correction); 2) experimental design (e.g., actor screening); 3) classification, which can be either supervised pattern recognition (e.g., discriminant analysis) or unsupervised pattern recognition (e.g., principal component analysis and cluster analysis) techniques; and 4) regression methods (e.g., artificial neural network, multiple linear regression, and partial least squares) [32, 40].

Pesticides have been broadly used in agricultural crops to control pests and microorganisms, providing many benefits for farmers, such as improvement of crop yields, quality, and value. However, improper or even proper application of pesticides can lead to contamination of environments, including water, soil, and air [15, 44]. Pesticide residues have been often found even in foods, and may be ultimately absorbed by the human body, impairing food safety and threatening human health. The inappropriate use of the pesticides may also leave residues in animal feeds, which could contaminate animal products for human consumption [28, 13]. Chlorpyrifos ($C_9H_{11}C_{13}NO_3PS$, CPF) containing a benzene ring is one of the most widely used organophosphate pesticides for agricultural products [30]. The application of CPF in agricultural production has been a concern due to its adverse effects on the environment and toxic effects on human beings, by inhibition of an enzyme (acetylcholinesterase) essential for nervous system function [12]. Aldicarb ($C_7H_{14}N_2O_2S$, ALD), in turn, is an oxime carbamate insecticide registered for use on a variety of crops, such as cotton, potatoes, peanuts, and others, but not approved for home and garden use [6, 39]. Like CPF, aldicarb inhibits cholinesterase and affects the nervous system, but the process is quickly reversible. It is believed that aldicarb is not carcinogenic or mutagenic, and does not cause other long-term adverse health effects [39]. Because of the potential significant adverse effects of CPF and ALD on the environment, animals, and humans, the regulatory agencies charged with regulation of pesticides established monitoring programs and statutory directives to control their use and applicability, imposing maximum residue limits (MRLs) in animal feeds and human foods [18]. The United States Environmental Protection Agency (EPA) established a tolerance for chlorpyrifos of 0.1 mg/kg for human and animal commodities [47, 12]. Recently, in Texas, two finished feed samples (poultry and beef cattle) were collected by

the Office of the Texas State Chemist, the local regulatory body for monitoring pesticide residues in animal feeds. They were found to be contaminated with high levels of CPF (0.48 mg/kg and 0.27 mg/kg). Of the follow-up samples, three (two poultry and one beef cattle) also contained CPF at 0.32 mg/kg, 0.01 mg/kg, and 0.14 mg/kg.

Analysis of CPF and ALD residues in animal feeds is not an easy task because a large amount of interfering co-extractants need to be removed and may significantly affect the performance of instruments and methods. Therefore, the extraction of CPF and ALD residues in animal feeds requires intricate strategies for efficient sample preparation and final determination [10, 49]. Of the methods applied for analysis of CPF and ALD in animal feeds, gas or liquid chromatography combined with mass spectroscopy have been routinely used [49, 16, 33, 39]. Although analytical methods based on enzyme-linked immunosorbent assays (ELISA) and biosensors have been developed to overcome some drawbacks of existing methods, such as time consuming, labor intensive, and expensive extraction and cleanup procedures, they are less attractive and reliable, particularly for rapid and accurate screening of pesticide contaminated feed samples having a variety of interferents due to inherent technical limitations and defects [19, 38, 51]. SERS may provide a more rapid and less expensive analytical method for animal feeds, because of the high selectivity and sensitivity required for practical applications. Previous studies reported the application of the SERS technique, with promising results for detection and identification of a few pesticide residues in diverse sample matrices [52], but rarely in animal feeds such as alfalfa, ground corn, fish meal, horse feed, swine feed, cattle feed, soy bean, and poultry feed. Therefore, the present study was aimed at investigating the feasibility of applying the SERS technique for direct detection and identification of CPF and ALD in animal feed, at different levels, to develop and validate the spectroscopic method for simple, non-destructive, and more efficient determination of residues of both pesticides.

2. Materials and Methods

2.1. Materials

Chlorpyrifos (CPF) and aldicarb (ALD) pesticides were obtained from Sigma-Aldrich (St. Louis, MO). $H AuCl_4 \cdot 3H_2O$ and trisodium citrate for synthesis of gold nanoparticle (AuNP) were also ordered from Sigma-Aldrich. All chemicals, organic solvents, and reagents were of analytical grade and used as received, without any further purification.

2.2. Sample Preparation

Animal feed samples naturally contaminated with CPF and ALD pesticides in a wide range of concentrations are not commercially obtainable. In addition, the pesticide residues are most likely inhomogeneously distributed in naturally-contaminated feed samples, which could influence the accuracy and repeatability in SERS measurement, particularly for low-concentration samples, and thus the reliability and predictability of the developed models. As a result, CPF- and ALD-free

beef cattle feeds were obtained from the Office of the Texas State Chemist (OTSC) regulatory samples and spiked with pesticide solutions to prepare samples in the range of 0 to 20 mg/kg and 0 to 100 $\mu\text{g}/\text{kg}$ for CFP and ALD, respectively. The spiked samples were placed in a polyethylene bottle and stored in a refrigerator at 4°C prior to SERS measurement and biochemical analysis. The samples were equilibrated at room temperature for more than 30 min before the next extraction process.

2.3. Sample Extraction and Chromatographic Analysis of CPF and ALD

CPF was extracted from the spiked sample based on the method described in a previous study [49]. Briefly, 5 g of the spiked sample were placed in a centrifuge tube to which 10 mL deionized water and 15 mL acetonitrile were added and vigorously shaken for 5 min. The resultant mixture was then added to 1 g trisodium citrate dihydrate, 0.5 g disodium hydrogen citrate sesquihydrate, 1 g sodium chloride, and 4 g anhydrous sodium sulphate, followed by hand shaking for 1 min. The tube was then centrifuged for 5 min at 700 g. After centrifugation, a 7.5-mL aliquot of supernatant was taken and mixed with 0.125 g primary secondary amine (PSA), 0.75 g anhydrous sodium sulphate, and 0.5 g C18. This mixture was further centrifuged for 5 min at 700g. An aliquot of the supernatant was directly used for SERS measurement or transferred into an amber vial for gas chromatography-mass spectrometry (GC-MS) analysis. For GC-MS analysis, 5 μL of the filtrate were injected into an Agilent 7890 GC (Agilent Technologies, Santa Clara, CA) coupled with an Agilent 5975 inert mass spectrometer using a Combi PAL autosampler (CTC Analytical, Zwingen, Switzerland). The temperature of the injection port was held at 250°C for 1.5 min and then increased to 300°C at 200°C/min. The final injection temperature was held for 20 min. The initial split mode was a split ratio of 20:1 and at 0.01 min, the split vent was closed and reopened at 1.5 min. Afterward, the split ratio was held at 100:1 for 20 min and reduced to 20:1 until the end of the run. The GC oven temperature was programmed as follows: initial temperature 80°C for 3 min, 80-150°C at 30°C/min, and 150-300°C at 10°C/min, which was held for 10 min. Helium was the carrier gas, at a constant flow rate of 1.2 mL/min. MS conditions were optimized to simultaneously obtain scan and a selected ion monitoring (SIM) data for quantitative determination of CPF. The characteristic ions monitored for quantitative analysis of CPF were m/z 197, 258, and 314, at a retention time of 16.5 min. Data acquisition and analysis were performed using Enhanced Chemstation (Agilent Technologies).

The method proposed by an earlier study [31] was used to extract ALD from the spiked feed sample. Briefly, 2.5 g of the spiked sample were first mixed with deionized water using a vortex. After soaking for 2 hr, the mixture was extracted with 15 mL of methanol containing 1% formic acid and shaken for 1 hr. Approximately 4 mL of the supernatant from the centrifugation at 1,600 g for 10 min were filtrated through a 0.25- μm syringe filter before SERS analysis and injected into the liquid chromatography tandem mass spectrometry (LC-MS/MS) system (Waters, Milford, MA). A Waters Acquit UPLC system was equipped with a 2.1 x 50 mm BEH C18 column (1.7- μm

particle size), operated at 50°C. The UPLC system was coupled to a Quattro Premier XE system with an electrospray interface (ESI). The mobile phases A and B were water with 20 $\mu\text{L}/\text{L}$ formic acid 1 mM ammonium formate and 95% methanol with 20 $\mu\text{L}/\text{L}$ formic acid and 1 mM ammonium formate, respectively. A Quattro Premier XE tandem quadrupole mass spectrometer system was operated under the following tuning settings: a source temperature of 120°C, a cone gas of 50 L/hr, a desolvation gas of 450 L/hr, a capillary voltage of 3.0 KV, extractor lens of 4 V, and desolvation temperature of 450°C. The multiple reaction monitoring (MRM) transition for ALD was m/z 208 (precursor ion) to m/z 89 (production ion).

2.4. Synthesis of Gold Nanoparticles

Gold nanoparticles (AuNP) for SERS measurements were prepared following the method of Bastús et al. [2] with minor modification. In brief, a three-necked flask containing 150 mL of 2.2 mM sodium citrate solution was heated under vigorous magnetic stirring and condensed for prevention of solvent evaporation. Once the solution started boiling, 1 mL of 25 mM HAuCl₄ was added and its color was changed as described in the previous study. The resultant solution containing particles with a size of ~10 nm as the Au seeds was used and cooled to 90°C. Then, 1 mL of 25 mM HAuCl₄ solution was added, and the solution was allowed to stand for 30 min to complete the reaction. After the reaction was complete, deionized water and 60 mM sodium citrate were added to dilute the extracted solution according to the predefined ratio of 60 mM sodium citrate:deionized water:sample extract = 2:53:55. The same process was repeated eight times to obtain AuNPs with a desirable particle size (~70 nm) (Figure 1).

A transmission electron microscopy (TEM) image and a size distribution of the synthesized AuNPs were obtained using JEOL 1200EX operating at a 100 kV (JEOL Ltd., Tokyo, Japan) and a Zetasizer Nano ZS ZEN3600 analyzer (Malvern Instrument Ltd, UK), respectively. The TEM image and particle size distribution results indicated that nanoparticles manufactured under effective control of temperature, pH, and seed particle concentration are monodispersed, with a narrow size distribution of mean diameter of <100 nm (Figure 1). Based on the particle size distribution, the zeta potential at neutral conditions was estimated as -35 eV, as proposed in other studies [48, 55].

2.5. SERS Measurement

A 30- μL portion of the AuNP solution was gently mixed with 10 μL of sample extract and 3 μL of 1 M NaCl solution to prepare the analyte mixture solution to acquire the SERS spectra. The resulting mixture solution was transferred to a centrifuge tube, vortexed until homogeneous, and allowed to cool to room temperature. Afterwards, 30 μL of the mixture solution were placed into an Al capsule and, after allowing the solution to stabilize for 1 min, the Al capsule was embedded in the well plate with a 7-mm diameter and a 10-mm depth mounted on the software-controlled motorized sample stage. The sample plate with 96 wells placed on a sample stage was automatically aligned at <2 micro step resolution, which would allow

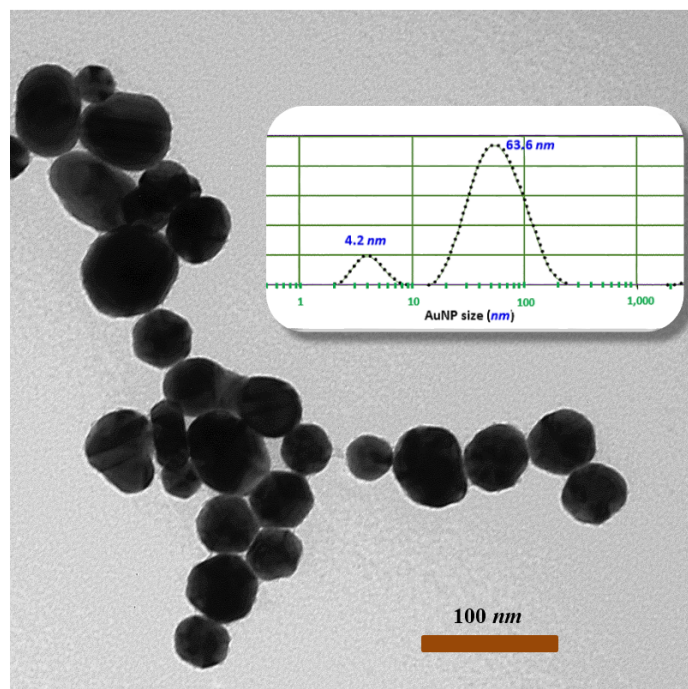


Figure 1: Transmission electron microscopy (TEM) image and a size distribution (inset) of gold nanoparticles (AuNPs) synthesized by kinetically controlled seeded growth procedure used for detection of CPF and ALD pesticide in animal feed

adjustment of the sample position in an x-y-z direction for optimal spectra acquisition. All samples were measured in triplicate using a Raman Spectroscopy system (RamanStation 400F, Perkin-Elmer, Beaconsfield, Buckinghamshire, UK). The Raman system was interfaced with the Spectrum software (v.6.3.) for data acquisition and analysis, and equipped with 350-mW near-infrared laser at an excitation wavelength of 785 nm and a 256 x 1024 pixel CCD detector. A total of 16 spots on each sample were scanned and averaged to obtain a representative spectrum of each sample. The sample was exposed to the laser power of about 20 mW with an exposure time of 15 sec and 2 scans, and its spectrum was recorded in the Raman shift range of 200 and 3500 cm^{-1} at the spectral resolution of 4 cm^{-1} .

2.6. Preprocessing of Spectral Data

Raw Raman spectra were preprocessed before data analysis and development of chemometric models because of unpredictable and inherent artifacts (e.g., cosmic rays, wavelength shift, broad band, aliasing effect, and increased noise) affecting the performance of Raman spectroscopy. Such artifacts can stem from subtle changes in environmental and instrumental conditions, including a drift of the monochromator or detector temperature, sample radiation, pixel variation, and grating shift [3]. As a result, the SERS spectrum of CPF and ALD samples was corrected for background at the time of spectral acquisition. The acquired raw spectrum was further baseline corrected and normalized to minimize the influence of the instrumental and environmental changes in the laboratory on the Raman signal and to reduce unpredictable variations in the laser energy and Raman signal. The normalized spectrum was further smoothed

using a 9-point Savitzky-Golay filtering function to calculate the first and second derivatives of the spectral data for removal of baseline and linear slope effects, and also deconvoluted for a higher resolution of unresolved Raman bands. All preprocessed spectral data were converted to ASCII file for further application of statistical procedures to develop qualitative and quantitative chemometric models.

2.7. Development and Validation of Chemometric Models

Multivariate statistical methods including component analysis (PCA), cluster analysis (CA), linear discriminant analysis (LDA), k-nearest neighbor (KNN), and partial least squares discriminant analysis (PLSDA) were applied on the preprocessed spectral data to develop chemometric models for classification of feed samples by the level of CPF and ALD spiking. All pesticide samples were assigned into one of five or six different subsets according to their spiking level prior to the statistical analyses. Two-thirds of spectral data ($n=108$ for CPF and $n=105$ for ALD) were used as a training dataset for development of the chemometric model, while the rest of the data ($n=36$ for CPF and $n=30$ for ALD) was considered as a validation dataset for validation of the developed model (Table 1). The performance, precision, and accuracy of the developed model were compared and evaluated mainly based on correction classification and false negative error rates to determine the model best suitable for analyzing pesticide-contaminated feed samples.

Similar to development of the qualitative chemometric models, the different preprocessed spectra were correlated with GC-MS reference values for development of quantitative calibration models by the use of multivariate statistical meth-

Pesticide	Dataset	Count (<i>n</i>)	Mean	Median	SD ^a	Kurtosis	Skewness
CPF ^b	Whole	144	3.68	0.80	5.90	2.18	1.85
	Training	108	3.70	0.80	5.92	2.38	1.88
	Validation	36	3.63	0.80	6.05	3.07	1.98
ALD ^c	Whole	135	20.33	7.00	29.70	1.88	1.77
	Training	105	20.33	7.00	29.87	2.07	1.80
	Validation	30	20.33	7.00	30.39	2.77	1.91

^aSD = standard deviation

^bCPF = chlorpyrifos

^cALD = aldicarb

^dThe units of mean, median, and SD are in mg/kg for CPF and $\mu\text{g}/\text{kg}$ for ALD.

Table 1: Descriptive statistics of feed samples spiked with known concentrations of CPF and ALD ^d

ods such as multiple linear regression (MLR), partial least squares regression (PLSR), and principal components regression (PCR). The total number of samples was also divided into a training and validation datasets at the same ratio as used for the qualitative models. The input variables (wavelengths) for MLR calibration models were determined using a stepwise regression and R^2 selection methods, while PLSR and PCR models were cross-validated using a leave-one out method for testing predictive ability of the models. All calibration models developed on different preprocessed data and statistical methods were evaluated and compared based on the root-mean-square error of calibration (RMSEC), the root mean standard error of prediction (RMSEP), and the correlation coefficient of determination (r^2), using external validation datasets. The lowest concentration at which the developed model can detect and quantify CPF and ALD in animal feed with reasonable accuracy and precision was determined by the limit of detection (LOD) and the limit of quantification (LOQ):

$$\text{LOD} = (|a| + 3S_a)/b \text{ and } \text{LOQ} = (|a| + 10S_a)/b,$$

where a is the intercept on the y -axis, S_a denotes the standard deviation for a , and b represents the slope of the linear regression curve.

Those chemometric methods were employed for this study because they have demonstrated their suitability and appropriateness in developing and validating the models to explain the relationship between acquired Raman spectra, chemical reference values and physicochemical properties in our previous studies [26, 27, 25]. More details on applied statistical techniques and their mathematical bases used for qualitative and quantitative models are described other studies [26, 9, 11, 20].

2.8. Statistical Analysis

Other statistical methods used for comparison between the model predicted and actual reference values include Pearson's correlation coefficient (r), a paired sample t-test, a significance of p -value, standard error of mean difference, and RPD value (the ratio of the standard deviation of the reference values to RMSEC). All statistical analyses and modeling for CPF and ALD analysis were carried out using SAS software (ver. 9.4,

SAS Institute, Cary, NC) and Microsoft Excel (Microsoft, Redmond, WA).

3. Results and Discussion

3.1. Spectra Data Processing and Analysis

Feed samples spiked with CPF had a narrower range of lower concentrations from 0 to 20 mg/kg with a mean of 3.68 mg/kg and a median of 0.8 mg/kg than ALD-spiked samples whose concentrations were in the range of 0 to 100 $\mu\text{g}/\text{kg}$ with a mean of 20.33 $\mu\text{g}/\text{kg}$ and a median of 7.0 $\mu\text{g}/\text{kg}$ (Table 1). Descriptive statistics of all training and validation datasets showed lower degree of peakedness (kurtosis of 2.18 to 3.07 for CPF and 1.88 to 2.77 for ALD) and left skewed distribution (skewness of 1.85 to 1.98 for CPF and 1.77 to 1.91 for ALD) of concentrations compared to normal distribution, regardless of the type of pesticide. The concentration ranges of CPF and ALD spiked samples used for the chemometric models developed in the present study were determined to cover the pesticide residues in animal feeds found in the commercial market and the feed supply chain [21, 1]. Therefore, the tested samples should be suitable and appropriate to develop the model for predicting and estimating the pesticide levels in animal feed products commonly found in the market and to assist in early detection and screening of the contaminated feed samples.

Figure 2 shows the average derivative preprocessed spectra of feed sample extracts representing each pesticide spiking group, displaying SERS spectral variations associated with CPF and ALD concentration in several Raman shift regions. Raman intensity difference was distinctive among the five or six groups of the pesticide spiked samples over the entire region of SERS spectra. Despite use of highly sensitive SERS technique, CPF samples with the range of higher concentrations (0 to 20 mg/kg) (Figure 2, A-D) displayed less pronounced and less significant spectral differences among the spiking groups compared to ALD samples with the range of lower concentration (0 to 100 $\mu\text{g}/\text{kg}$) (Figure 2, E-H). This can be explained, in part, by the narrower range of spiking concentrations and the influence of less compatible morphological and chemical properties of CPF of larger molecular weight (350.59 g/mol) with SERS active sites than ALD, of smaller molecular weight (190.26 g/mol), lowering Raman signal enhancement. Irrespective of the type

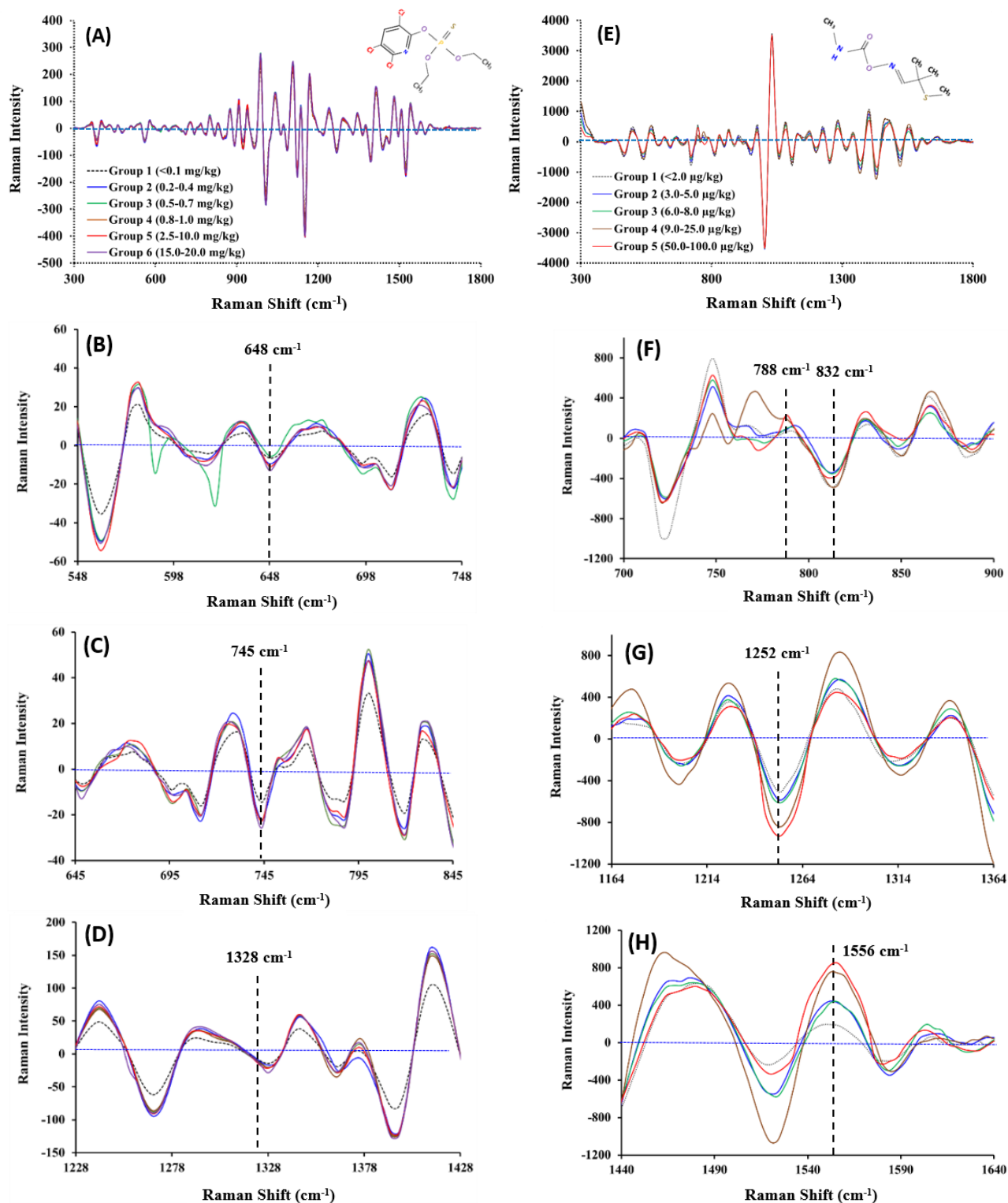


Figure 2: Raman characteristic peaks of the average 2nd derivative preprocessed spectra of chlorpyrifos (CPF) samples at 648 cm^{-1} (P=S stretching), 745 cm^{-1} (C-Cl stretching), and 1328 cm^{-1} (C-N stretching) (A-D) and those of the average 1st derivative spectra of aldicarb (ALD) samples at 788 cm^{-1} (N-H deformation), 832 cm^{-1} (N-O stretching), 1252 cm^{-1} (N=S=O antisymmetric stretching), and 1556 cm^{-1} (CNH stretching-bending) (E-H)

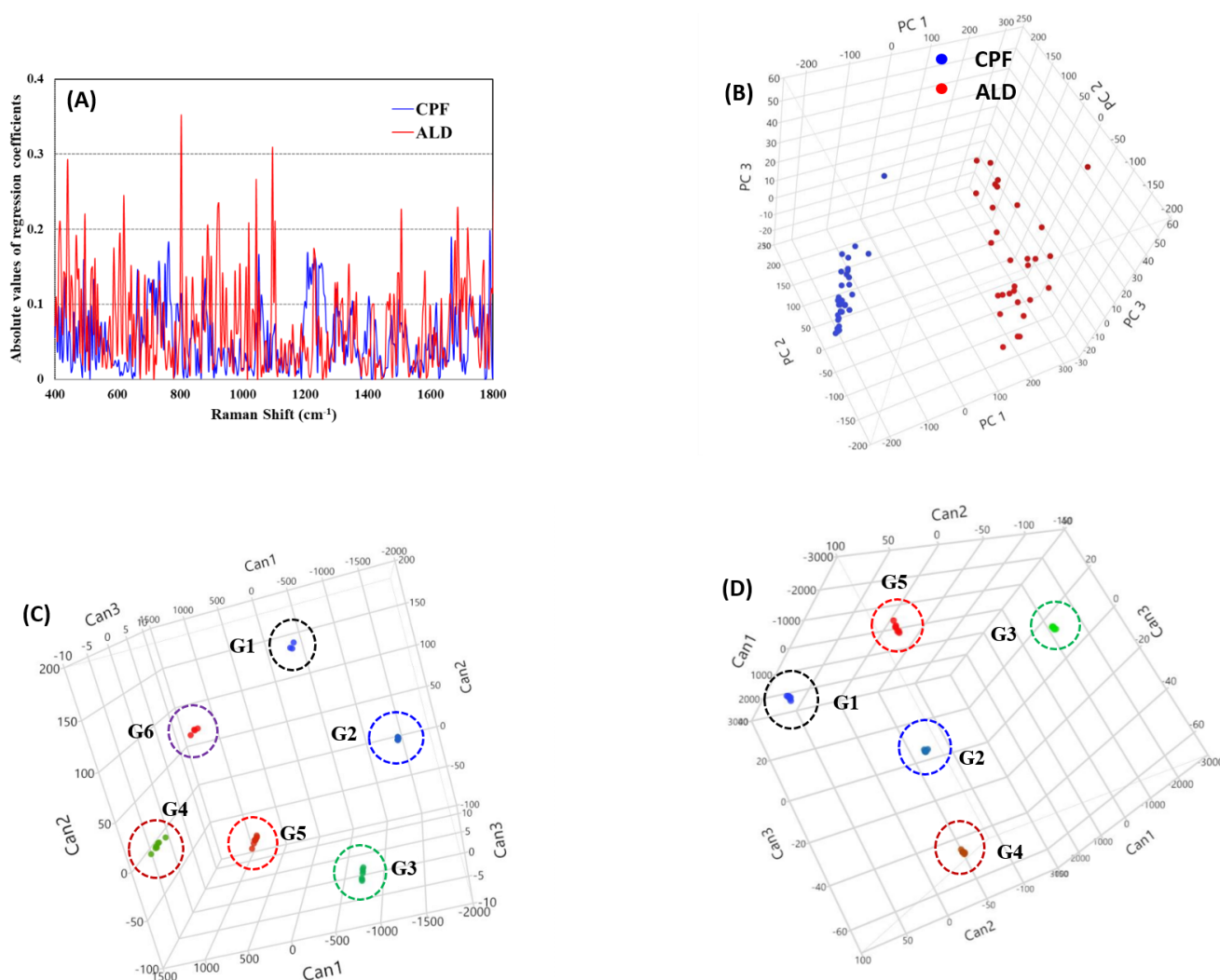


Figure 3: Absolute correlation coefficients of PLSR models developed on SERS spectra (A), and the scatter plots created by the principle component scores (B) and canonical discriminant scores (C and D) for different CPF and ALD spiking groups

of pesticide, Raman intensity difference appeared to be less distinctive in some Raman shift regions among the spiking groups, which could be caused by a similar level of coexisting functional chemical groups in samples. There were several Raman shift regions showing significant spectral difference in Raman intensity, which could be attributed to the presence of different concentrations of pesticides in feed samples. Raman shift regions that are apparently closely associated with CPF concentration in feed samples include $636\text{-}964\text{ cm}^{-1}$ and $1268\text{-}1412\text{ cm}^{-1}$, while ALD concentrations in feed samples seem to be correlated with several Raman bands in Raman shift regions of $704\text{-}952\text{ cm}^{-1}$, $1200\text{-}1316\text{ cm}^{-1}$, and $1432\text{-}1588\text{ cm}^{-1}$ (Figure 2). Compared to normalized spectra, 1st and 2nd derivative preprocessed spectra showed a slightly better separation of the spiked feed samples at different concentrations of CPF and ALD. In the derivative preprocessed spectra, the degree of Raman intensity difference among the pesticide spiking groups was significantly dependent on the spiking level, although it was often not visualized between the groups with a small difference in pesticide

concentration.

The characteristic peaks of CPF and ALD were clearly identified with synthesized SERS substrates. Although SERS substrates did not show a high efficiency in predicting very lower concentrations of CPF and ALD in samples, the Raman signal appeared to be enhanced with a further increase of pesticide concentration up to the highest concentration employed for the study. Raman peaks highly correlated with and proportional to pesticide concentration also showed higher correlation coefficients, regression coefficients of PLS models, and factor loadings in PCA for the concentrations (Figure 3). The vibrational modes of functional chemical groups corresponding to the characteristic peaks of CPF and ALD could be tentatively determined based on a spectroscopy software (KnowItAll®, Bio-Rad, Hercules, 412 CA) and previous studies [26, 5, 42]. The characteristic peaks of CPF at 648 cm^{-1} , 745 cm^{-1} , and 1328 cm^{-1} are attributed to P=S stretching, C-Cl stretching, and C-N stretching, respectively (Figure 2, A-D). The prominent peaks of ALD at 788 cm^{-1} , 832 cm^{-1} , 1252 cm^{-1} , and 1556 cm^{-1}

Pesticide	Group	Training Dataset ^a		Validation Dataset ^b			
		Actual	Prediction	Actual	KNN ^c	LDA ^d	PLSDA ^e
CPF ^f	1 (<0.1 mg/kg)	9	9	6	6	6	6
	2 (0.2-0.4 mg/kg)	21	21	6	2	2	3
	3 (0.5-0.7 mg/kg)	21	21	6	0	0	0
	4 (0.8-1.0 mg/kg)	21	21	6	6	6	6
	5 (2.5-10.0 mg/kg)	24	24	6	3	3	0
	6 (15.0-20.0 mg/kg)	12	12	6	6	6	3
	Total (% correct)	108	108 (100)	36	23 (63.9)	23 (63.9)	18 (50.0)
ALD ^g	1 (<2.0 µg/kg)	21	21	6	6	6	6
	2 (3.0-5.0 µg/kg)	21	21	6	6	6	2
	3 (6.0-8.0 µg/kg)	21	21	6	4	4	3
	4 (9.0-25.0 µg/kg)	21	21	6	4	4	4
	5 (50.00-100.0 µg/kg)	21	21	6	3	3	1
	Total (% correct)	105	105 (100)	30	23 (76.7)	23 (76.7)	16 (53.3)

^aAll chemometric models applied on the training datasets classified pesticide spiked samples into the predefined groups with 100% correct classification rate.

^bThe columns of KNN, LDA, and PLSDA represent the number of correctly classified samples of each pesticide.

^cKNN = k-nearest neighbor

^dLDA = linear discriminant analysis

^ePLSDA = partial least squares discriminant analysis

^fCPF = chlorpyrifos

^gALD = aldicarb

Table 2: Descriptive statistics of feed samples spiked with known concentrations of CPF and ALD

correspond to the N-H deformation, N-O stretching, N=S=O antisymmetric stretching, and CNH stretching-bending, respectively (Figure 2, E-H). These findings indicate that SERS spectral response is sensitive and specific enough to measure variations in concentrations of CPF and ALD in feed sample extracts. The SERS spectra of CPF- and ALD-spiked samples showed some major peaks which are also found in standard solid CPF and ALD by standard Raman spectroscopy. However, SERS and standard Raman spectroscopy did not seem to share identical spectral features, likely due to different sensitivity to the pesticide molecules, peak shifts in SERS spectra, and interference by a large number of compounds extracted from the feed sample. An identification of the fingerprint regions for pesticide molecules appeared to be somewhat difficult for animal feeds compared to other matrices, because interference and contribution from functional chemical groups of coextractants seemed to have a huge impact on the Raman signal of CPF and ALD molecules, thus predominating over their fingerprint regions [5, 29, 41]. In addition, inhomogeneous distribution of gold nanoparticles and competition for binding to the active surface sites of SERS substrates between coextractants and pesticide molecules may also have an adverse effect on enhancement and easy identification of Raman signals of the target molecules. Other studies reported that the intensity of the UV-VIS plasmon absorption band was proportional to the size of the nanoparticles [2]. Since inhomogeneous distribution of AuNPs in size could cause uneven distribution of hot spots and active surfaces on the nanoparticles and their assemblies, interacting with the pesticide molecules and their chemical functional groups, the inhomogeneity of the particle size

distribution may greatly affect the consistency of the Raman enhancement effect and the repeatability of the Raman signal intensity [27, 2].

3.2. Development and Validation of Chemometric Classification Models

The classification models to classify and predict CPF and ALD spiked samples into predefined groups at different concentrations were developed on the preprocessed spectra data by applying the chemometric methods mentioned above. The classification accuracies of the applied discriminant models for SERS spectra data are presented in Table 2. KNN and LDA models showed higher predictive accuracy and lower prediction error for training and external validation datasets than the PLSDA model. Regardless of the preprocessed and chemometric method applied, all three models showed a correct classification rate of 100 percent by the resubstitution method of error estimation, which typically gives an optimistic error rate [20].

KNN models for CPF and ALD developed on a training dataset demonstrated a high classification accuracy of 100 percent in cross-validation analysis for all preprocessed data when all variables and a subset of variables selected using a stepwise selection in PROC STEPDISC procedure were applied. However, the correct classification rate of LDA and PLSDA models was significantly lower with all variables applied to the training dataset (Table 2). When the calibration models were applied on an external validation dataset, both the KNN and LDA models showed identical and somewhat lower classification accuracies, around 65 percent for CPF and 75 percent for ALD. Despite the lower accuracy for the validation

	CPF ^a			ALD ^b		
	MLR ^c	PCR ^d	PLSR ^e	MLR	PCR	PLSR
<i>Slope:</i>						
Training	0.982	0.466	0.969	0.968	0.616	0.963
Validation	1.002	0.202	0.873	0.908	0.350	0.878
LOD ^f	1.4	26.9	2.0	9.0	77.4	10.0
LOQ ^g	4.2	43.2	3.9	24.4	154.0	28.1
RMSEC ^h	0.793	4.259	1.030	5.246	18.193	5.637
RMSEP ⁱ	2.338	5.514	2.294	11.091	29.695	12.746
<i>r</i> ^j	0.929	0.405	0.925	0.927	0.446	0.904
SE Mean ^k	0.34	0.49	0.33	1.64	3.60	1.88
RPD ^l	2.53	1.07	2.58	2.68	1.05	2.33

^aCPF = chlorpyrifos

^bALD = aldicarb

^cMLR = multiple linear regression

^dPCR = principal component regression

^ePLSR = partial least squares regression

^fLOD = limit of detection

^gLOQ = limit of quantitation

^hRMSEC = root-mean-square error of calibration

ⁱRMSEP = root-mean-square error of prediction

^j*r* = Pearson correlation coefficient

^kSE Mean = standard error of the mean difference between actual and predicted values of the external validation dataset

^lRPD = ratio of the standard deviation of reference values to the standard error of cross-validation values

^mThe units of LOD, LOQ, RMSEC, RMSEP, and SE Mean are in mg/kg for CPF and $\mu\text{g}/\text{kg}$ for ALD.

Table 3: Statistical analysis results of three chemometric models for SERS spectral data in predicting CPF and ALD concentration in animal feed extracts^m

dataset, the chemometric models did not misclassify any moderate or high CPF and ALD concentration samples to Group 1 (very low or free of pesticide), that is, no false negative results. The zero-misclassification of pesticide spiked samples as negative is meaningful and crucial in analyzing commercial and non-commercial samples, implying that the SERS technique can be used as a simple and reliable tool for a rapid and accurate screening of pesticide-contaminated samples for a high-throughput analysis to ensure feed safety. The dendrogram from cluster analysis and the scatter plot created using the first few principal components with higher eigenvalues showed a clear separation of a different type of pesticide for all pre-processed spectral data (Figure 3). However, the classification of the pesticide-spiked samples within each pesticide was not clearly configured in the dendrogram and scatter plot by the groups at different concentrations, even when the best clustering algorithm (hierarchical Ward's minimum variance method) and more principal components were applied.

Unlike inaccurate clustering of pesticide-spiked samples to the predefined groups on the principal component scatter plot, the first few canonical discriminant variables, each of which is a combination of the original variables, allowed to clearly sep-

arate the spiking groups by pesticide concentration on a scatter plot [20]. Figure 3 shows the scatter plot created by canonical discriminant scores obtained from LDA for SERS spectra, and exhibited actual distance and difference in spectral characteristics among different spiking groups in a reduced dimensional space. The 3D scatter plot was generally in good agreement with the classification results of the models, and appeared to clearly group CPF- and ALD-spiked samples at a similar level of pesticide within the same group closely together, while the samples with very different concentrations are grouped at larger distance from each other. The first three canonical variables were significant ($p < 0.01$) and substantially contributed to discrimination and prediction of the predefined groups. A total of more than 90 percent of variation in all processed spectra could be explained by the first three canonical variables.

3.3. Development and Validation of Chemometric Quantification Models

Three chemometric methods, including multiple linear regression (MLR); partial least squares regression (PLSR); and principal component regression (PCR); were applied to build the calibration models for CPF and ALD quantification in animal feed, using all preprocessed spectral data at a Raman shift

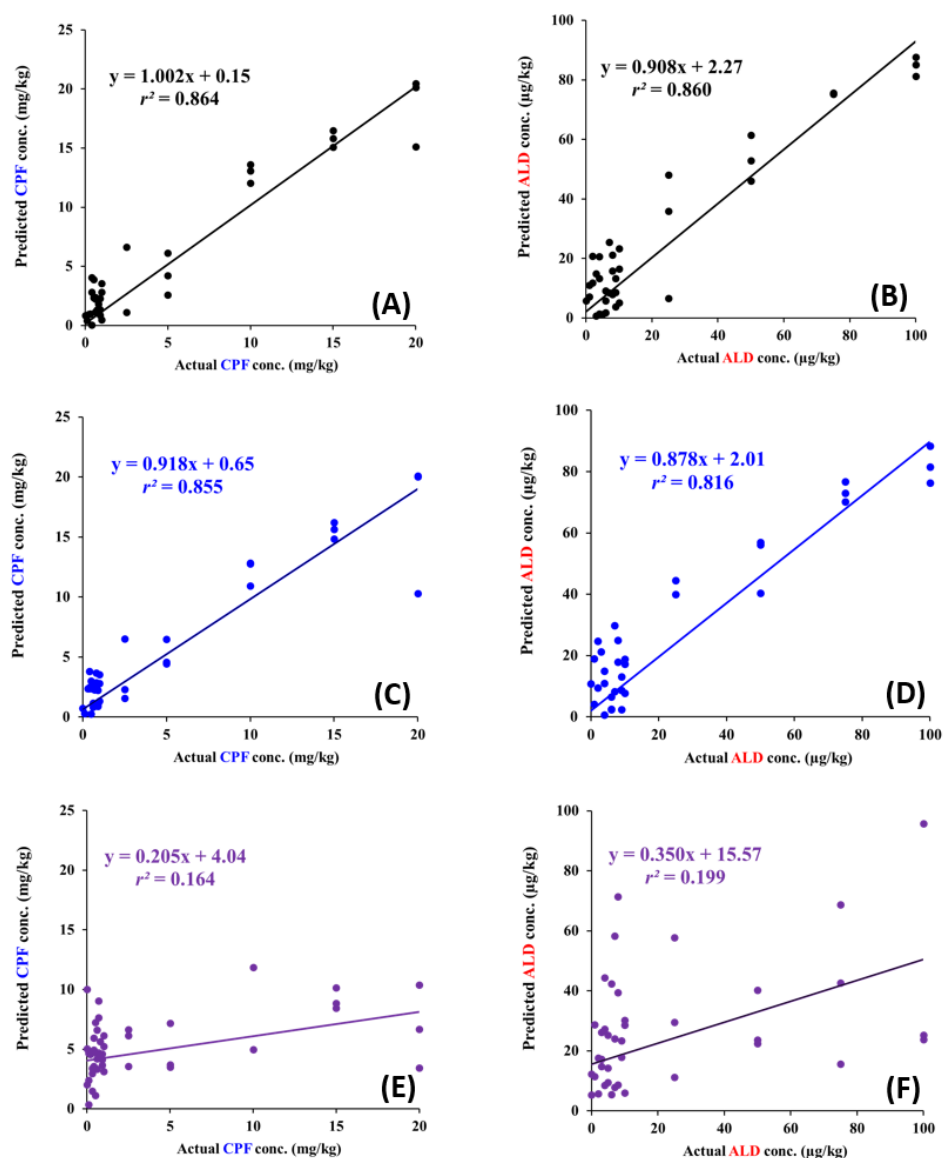


Figure 4: Linear regression plots of three chemometric models developed on spectral data and applied on the external validation datasets, showing the relationship between predicted values by the models and actual values determined by the reference methods for chlorpyrifos (CPF) and aldicarb (ALD) analysis: (A, B) MLR, multiple linear regression; (C, D) PLSR, partial least squares regression; and (E, F) PCR, principal component regression

range of 400 to 2500 cm^{-1} . These chemometric methods were useful and suitable to explain the relationship and differentiate between pesticide-contaminated and non-contaminated samples by extracting meaningful information from highly overlapped and superimposed Raman spectra with subtle difference [27, 24, 43].

Table 3 and Figure 4 show the results of chemometric models for SERS spectral data to compare SERS predicted values by the models to actual CPF and ALD values determined by the reference methods. The results indicate that the performance of the models were slightly or significantly influenced by the type of pesticide and chemometric method applied. MLR and PLSR models for CPF and ALD quantification performed bet-

ter than PCR models, exhibiting lower error rate, better regression quality, and higher predictability, which, in fact, was consistent with our previous studies [26, 27]. The MLR models for ALD quantification performed slightly better according to r^2 values (0.860 vs 0.816) and predictive error rates (11.091 $\mu\text{g}/\text{kg}$ vs 12.746 $\mu\text{g}/\text{kg}$) than PLSR models, while the two models were very comparable in predicting CPF concentration in animal feed with respective r^2 values of 0.864 vs 0.855 and respective error rates of 2.338 mg/kg and 2.294 mg/kg. The PCR models for CPF and ALD quantification were less satisfactory compared to MLR and PLSR models (Table 3 and Figure 4). The lower predictive power and performance of PCR models, regardless of the type of pesticide, can be attributed in part to

the principle of the PCR algorithm, which is a procedure to decompose the acquired spectral data for variance estimation. As a result, the PCR algorithm can be less powerful and accurate in developing the model for quantitative analysis than the PLSR algorithm, which calculates the covariance between the acquired spectra and actual concentrations of pesticides in samples. In the present study, the SERS spectra were not highly resolved and reproducible due to several possible reasons mentioned above, which could more significantly influence the performance of the PCR algorithm than other chemometric algorithms.

The subset of the optimum wavelengths was selected as input variable in MLR models by testing all possible combinations of Raman wavelengths and eliminating overfitting of the model and collinearity of highly correlated wavelengths, using the stepwise regression variable selection procedure and the adjusted R^2 method to best predict CPF and ALD concentration [27, 4]. MLR models developed on preprocessed spectral data showed higher coefficients of determination (r^2) and lower error rate (RMSEC and RMSEP) and explained a high degree of variation in the spectral data. MLR calibration models applied to training datasets of SERS spectral data showed acceptable predictability, with r^2 value of 0.982 and RMSEC of 0.793 mg/kg for CPF and also r^2 values of 0.968 and RMSEC of 5.266 $\mu\text{g}/\text{kg}$ for ALD. When MLR calibration models were further tested for the external validation datasets, the models displayed lower predictive accuracy (r^2 values of 0.864 for CPF and 0.860 for ALD) and moderate error rates (RMSEP values of 2.338 mg/kg for CPF and 11.091 $\mu\text{g}/\text{kg}$ for ALD). The slopes of MLR calibration models for training and validation datasets were 0.982 and 1.002 for CPF, respectively. Likewise, the MLR calibration models for ALD quantification displayed slopes of 0.968 for training dataset and 0.908 for validation dataset (Table 3). These statistical results are promising, indicating that highly reliable and robust MLR models on SERS spectra can be developed under optimal spectral sampling conditions and through innovative approaches for better predicting CPF and ALD concentration in animal feed. Raman wavelengths used as input variables in MLR models were associated with functional chemical groups of pesticides spiked in samples. These wavelengths also showed higher absolute correlation coefficients for PLSR models (Figure 3), indicating the selected wavelengths are more critical and meaningful in quantifying CPF and ALD concentration in animal feed. However, MLR models were inaccurate and rather unreliable in predicting lower CPF concentrations of less than 1.5 mg/kg and ALD concentrations of less than 10.0 $\mu\text{g}/\text{kg}$, displaying higher prediction errors (Figure 4). The obtained limit of detection (LOD) and the limit of quantitation (LOQ) of the MLR models also showed a little higher values than the maximum residue limits (MRLs) (Table 3). These are also true for other chemometric models, particularly PCR models, which are believed unable to properly predict the lower pesticide concentration residues in animal feed. The disparity between model predicted and reference values at lower CPF and ALD concentrations may be attributed to several factors: 1) Raman laser is not sufficiently powerful (considered to reach only a few micrometers below the sample surface), so

it may not penetrate deeply enough in animal feed extracts to detect a gradient of pesticides; 2) pesticide molecules adsorbed on or in the vicinity of nanoparticles are inhomogeneously distributed and vary from sample to sample; and 3) nanoparticle size is not uniform and the agglomeration of nanoparticles easily occurs in some areas, deteriorating the repeatability of the spectra [26, 34, 24].

Similar to the multivariate regression method of PCR, PLSR is a quantitative regression algorithm that uses a few factors enabling it to contain almost all information from the original Raman spectra [36]. The optimum number of factors was determined based on the predicted residual error sum of squares (PRESS) and p-value of comparing the model between two different numbers of extracted factors [27]. In this study, PLSR models for SERS spectral data required eight and five factors to predict CPF and ALD concentration in animal feed, respectively, while PCR models for the same spectral data required 10 factors for CPF quantification and 15 for ALD quantification. Requiring fewer factors by PLSR models indicates that the PLSR algorithm is a more powerful technique for prediction of pesticide concentration [27, 8, 36]. PLSR models developed with different number of factors exhibited similar performance and predictability for predicting CPF and ALD concentration (Table 3 and Figure 4). In PLSR models, the models for CPF quantification applied to training and validation datasets of SERS spectra yielded moderate r^2 values (>0.850), lower error rates of RMSEC (1.030 mg/kg) and RMSEP (2.294 mg/kg), and a linear regression slope in the range of ~ 0.9 . Likewise, the PLSR calibration models developed with ALD-spiked samples with lower concentrations than CPF samples showed equal predictive accuracy and acceptable sensitivity to the PLSR models for CPF, with comparable r^2 values, moderately low error rates, and linear regression slopes slightly lower than 0.9 (Table 3 and Figure 4). The PCR calibration models applied to the validation datasets of SERS spectral data yielded much less predicting ability ($r^2=0.164$ and RMSEP=5.514 mg/kg for CPF and $r^2=0.199$ and RMSEP=29.695 $\mu\text{g}/\text{kg}$ for ALD) to quantify CPF and ALD concentration, compared to MLR and PLSR models. In addition to some reasons described earlier, the poor performance of the PCR models irrespective of the type of pesticide and preprocessing method can be explained also by similar spectral properties of the samples, poor repeatability of spectra, and interference of pesticide Raman bands from other coextractants.

CPF and ALD concentrations predicted by the three chemometric models found no statistically significant difference when compared with actual values determined by standard wet-chemical methods ($p>0.01$). The standard errors of paired difference between the predicted and reference values were comparable between MLR and PLSR models and higher in PCR models for CPF and ALD quantification (Table 3). In the Pearson's correlation coefficient comparison, the predicted values by the MLR and PLSR models developed on SERS spectra were highly correlated with reference values ($r>0.925$ for CPF and $r>0.904$ for ALD), indicating equivalent results to the chromatographic methods at the pesticide levels tested, while those by PCR models were poorly correlated with the refer-

ence values ($r=0.405$ for CPF and $r=0.446$ for ALD). RPD values calculated by standardizing RMSEP values against standard deviation of the reference values in the external validation dataset for SERS spectral data were 2.53 and 2.68 for CPF and ALD in MLR models, respectively. Likewise, RPD values of PLSR models showed greater than 2.3 for CPF and ALD samples, while PCR models developed on SERS spectral data of the pesticide samples did not exceed RPD values of 2.0. The RPD results indicate that MLR and PLSR may be semi-quantitative and effective for screening CPF and ALD pesticide-contaminated feed samples.

Apparently, there have been little attempts to develop SERS methods for detection of CPF and ALD residues in animal feed. Our results of chemometric models for predicting the pesticide concentration in animal feed are equivalent or even surpassing those reported in previous studies using other sample matrices, in terms of predictive accuracy and error rates. The findings and implications from the present study clearly demonstrate the potential feasibility of the SERS technique as more effective and efficient analytical tool for CPF and ALD quantification in animal feed than standard wet-chemical methods with respect to cost-effectiveness, simplicity, and rapidness in analytical procedure, environmental cleanness, general applicability, and rapid growth in the pace of technical improvement.

4. Conclusions

The current research successfully demonstrated the potential feasibility of a SERS-based spectroscopic method, and also its challenges, as a rapid, simple, and cost-effective analytical tool for early detection and screening of chlorpyrifos- and aldicarb-contaminated animal feed. The selected chemometric models exhibited a satisfactory predictive capacity and performance on pesticide-spiked samples in qualitative and quantitative analysis, which may help reduce significantly the risk of animal feed hazard imposed by pesticide contamination, although accurate quantitative determination of low-pesticide concentration samples is still challenging, and more simplified sample preparation with minimum effort and low cost needs to be implemented for on-site analysis. The SERS-based spectroscopic method could offer critical advantages and benefits, with plenty of information about samples, over conventional wet-chemical methods for selected pesticide analysis, perhaps suitable for rapid, real-time monitoring and onsite analysis of contaminated feed samples. However, broader application of the SERS technique might be hindered by several technical difficulties and constraints, including lack of stable Raman laser source, interference of biological fluorescence, insensitivity to a target analyte in the low concentration range, expensive nanomaterials, and poor repeatability and reproducibility of spectra induced by instability of nanostructure and inconsistent concentration of nanoparticles in different batches. Nevertheless, the SERS spectroscopic method is promising if it can improve its predictive capacity and applicability through adoption of new technologies and innovative approaches, such as development of inexpensive laser source and signal detection system, simplification of data processing and interpretation, development of

new algorithms and statistical techniques for effective removal of noise and redundant information, production of low-cost nanoparticles, and development of highly efficient system components. Therefore, the proposed SERS spectroscopic method and its further modified version can be considered in the future as a more powerful and economical analytical tool than any other methods for CPF and ALD analysis in animal feed, to improve the quality and safety of food and feed products and thus protect human and animal health.

5. Declaration of Conflicting Interest

The authors declare no conflicts of interest.

6. Acknowledgement

The authors wish to acknowledge the financial support, data sharing, and other valuable assistance provided for this research by the Office of the Texas State Chemist, Texas A&M AgriLife Research, Texas A&M University.

7. Article Information

This article was received December 2, 2019, in revised form April 5, 2020, and made available online August 30, 2020.

8. References

- [1] Baron, R. L., & Merriam, T. L. (1988). Toxicology of Aldicarb. In G. W. Ware (Ed.), *Reviews of Environmental Contamination and Toxicology* (Vol. 105, pp. 1-70). Springer. doi: 10.1007/978-1-4612-3876-8_1
- [2] Bastús, N. G., Comenge, J., & Puentes, V. (2011). Kinetically Controlled Seeded Growth Synthesis of Citrate-Stabilized Gold Nanoparticles of up to 200 nm: Size Focusing versus Ostwald Ripening. *Langmuir*, 27(17), 11098-11105. doi: 10.1021/la201938u
- [3] Bowie, B. T., Chase, D. B., & Griffiths, P. R. (2000). Factors Affecting the Performance of Bench - Top Raman Spectrometers. Part I: Instrumental Effects. *Applied Spectroscopy*, 54(5), 164A-173A. doi: 10.1366/0003702001949924
- [4] Broadhurst, D., Goodacre, R., Jones, A., Rowland, J. J., & Kell, D. B. (1997). Genetic algorithms as a method for variable selection in multiple linear regression and partial least squares regression, with applications to pyrolysis mass spectrometry. *Analytica Chimica Acta*, 348(1-3), 71-86. doi: 10.1016/S0003-2670(97)00065-2
- [5] Chen, Z., Yongyu, L., Yankun, P., & Tianfeng, X. (2015). Detection of chlorpyrifos in apples using gold nanoparticles based on surface enhanced Raman spectroscopy. *International Journal of Agricultural and Biological Engineering*, 8(5), 113-120. doi: 10.3965/j.ijabe.20150805.1771
- [6] Choudhary, S., Yamini, Raheja, N., Yadav, S. K., Kamboj, ML., & Sharma, A. (2018). A review: Pesticide residue: Cause of many animal health problems. *Journal of Entomology and Zoology Studies*, 6(3), 330-333.
- [7] Craig, A. P., Franca, A. S., & Irudayaraj, J. (2013). Surface-Enhanced Raman Spectroscopy Applied to Food Safety. *Annual Review of Food Science and Technology*, 4, 369-380. doi: 10.1146/annurev-food-022811-101227
- [8] Cramer, R. D., III. (1993). Partial Least Squares (PLS): Its strengths and limitations. *Perspectives in Drug Discovery and Design*, 1, 269-278. doi: 10.1007/BF02174528
- [9] Delwiche, S. R., & Hareland, G. A. (2004). Detection of Scab-Damaged Hard Red Spring Wheat Kernels by Near-Infrared Reflectance. *Cereal Chemistry*, 81(5), 643-649. doi: 10.1094/CCHEM.2004.81.5.643

- [10] Di Ottavio, F., Pelle, F. D., Montesano, C., Scarpone, R., Escarpa, A., Compagnone, D., & Sergi, M. (2017). Determination of Pesticides in Wheat Flour Using Microextraction on Packed Sorbent Coupled to Ultra-High Performance Liquid Chromatography and Tandem Mass Spectrometry. *Food Analytical Methods*, 10, 1699-1708.
- [11] Dowell, F. E., Pearson, T. C., Maghirang, E. B., Xie, F., & Wicklow, D. T. (2002). Reflectance and Transmittance Spectroscopy Applied to Detecting Fumonisin in Single Corn Kernels Infected with *Fusarium verticillioides*. *Cereal Chemistry*, 79(2), 222-226. doi: 10.1094/CCHEM.2002.79.2.222
- [12] Eaton, D. L., Daroff, R. B., Autrup, H., Bridges, J., Buffler, P., Costa, L. G., Coyle, J., McKhann, G., Mobley, W. C., Nadel, L., Neubert, D., Schulte-Herrmann, R., & Spencer, P. S. (2008). Review of the Toxicology of Chlorpyrifos With an Emphasis on Human Exposure and Neurodevelopment. *Critical Reviews in Toxicology*, 38(sup2), 1-125. doi: 10.1080/10408440802272158
- [13] Fagnani, R., Beloti, V., Battaglini, A. P., Dunga, K. D., & Tamanini, R. (2011). Organophosphorus and carbamate residues in milk and feedstuff supplied to dairy cattle. *Pesquisa Veterinária Brasileira*, 31(7), 598-602. doi: 10.1590/S0100-736X2011000700009
- [14] Fan, M., Andrade, G. F. S., & Brolo, A. G. (2011). A review on the fabrication of substrates for surface enhanced Raman spectroscopy and their applications in analytical chemistry. *Analytica Chimica Acta*, 693(1-2), 7-25. doi: 10.1016/j.aca.2011.03.002
- [15] Fernandez-Alvarez, M., Llompарт, M., Lamas, J. P., Lores, M., Garcia-Jares, C., Cela, R., & Dagnac, T. (2008). Simultaneous determination of traces of pyrethroids, organochlorines and other main plant protection agents in agricultural soils by headspace solid-phase microextraction-gas chromatography. *Journal of Chromatography A*, 1188(2), 154-163. doi: 10.1016/j.chroma.2008.02.080
- [16] Garrido-Frenich, A., Arrebola, F. J., González-Rodríguez, M. J., Vidal, J. M., & Diez, N. M. M. (2003). Rapid pesticide analysis, in post-harvest plants used as animal feed, by low-pressure gas chromatography-tandem mass spectrometry. *Analytical and Bioanalytical Chemistry*, 377(6), 1038-1046. doi: 10.1007/s00216-003-2167-8
- [17] Gautam, R., Vanga, S., Ariese, F., & Umapathy, S. (2015). Review of multidimensional data processing approaches for Raman and infrared spectroscopy. *EPJ Techniques and Instrumentation*, 2(8). doi: 10.1140/epjti/s40485-015-0018-6
- [18] González-Curbelo, M. A., Herrera-Herrera, A. V., Ravelo-Pérez, L. M., & Hernández-Borges, J. (2012). Sample-preparation methods for pesticide-residue analysis in cereals and derivatives. *TrAC Trends in Analytical Chemistry*, 38, 32-51. doi: 10.1016/j.trac.2012.04.010
- [19] Huang, S., Hu, J., Liu, M., Wu, R., & Wang, X. (2017). Density Functional Theory Calculation and Raman Spectroscopy Studies of Carbamate Pesticides (in Chinese). *Guang Pu Xue Yu Guang Pu Fen Xi*, 37(3).
- [20] Johnson, D. E. (1998). Discriminant analysis. In D. E. Johnson (Ed.), *Applied Multivariate Methods for Data Analyst* (pp. 217-285). Duxbury Press.
- [21] Kan, C. A., & Meijer, G. A. L. (2007). The risk of contamination of food with toxic substances present in animal feed. *Animal Feed Science and Technology*, 133(1/2), 84-108. doi: 10.1016/j.anifeeds.2006.08.005
- [22] Kim, A., Barcelo, S. J., & Li, Z. (2014). SERS-based pesticide detection by using nanofinger sensors. *Nanotechnology*, 26(1), 015502. doi: 10.1088/0957-4484/26/1/015502
- [23] Kim, J., Hwang, J., & Chung, H. (2008). Comparison of near-infrared and Raman spectroscopy for on-line monitoring of etchant solutions directly through a Teflon tube. *Analytica Chimica Acta*, 629(1-2), 119-127. doi: 10.1016/j.aca.2008.09.032
- [24] Kos, G., Lohninger, H., Mizaiakoff, B., & Krška, R. (2007). Optimisation of a sample preparation procedure for the screening of fungal infection and assessment of deoxynivalenol content in maize using mid-infrared attenuated total reflection spectroscopy. *Food Additives and Contaminants*, 24(7), 721-729. doi: 10.1080/02652030601186111
- [25] Lee, K-M., Armstrong, P. R., Thomasson, J. A., Sui, R., Casada, M., & Herrman, T. J. (2010). Development and Characterization of Food-Grade Tracers for the Global Grain Tracing and Recall System. *Journal of Agricultural and Food Chemistry*, 58(20), 10945-10957. doi: 10.1021/jf101370k
- [26] Lee, K-M., & Herrman, T. J. (2016). Determination and Prediction of Fumonisin Contamination in Maize by Surface-Enhanced Raman Spectroscopy (SERS). *Food and Bioprocess Technology*, 9, 588-603. doi: 10.1007/s11947-015-1654-1
- [27] Lee, K-M., Herrman, T. J., Bistrat, Y., & Murray, S. C. (2014). Feasibility of Surface-Enhanced Raman Spectroscopy for Rapid Detection of Aflatoxins in Maize. *Journal of Agricultural and Food Chemistry*, 62(19), 4466-4474. doi: 10.1021/jf500854u
- [28] Leeman, W. R., Van Den Berg, K. J., & Houben, G. F. (2007). Transfer of chemicals from feed to animal products: The use of transfer factors in risk assessment. *Food Additives and Contaminants*, 24(1), 1-13. doi: 10.1080/02652030600815512
- [29] Liu, Y., & Liu, T. (2010). Determination of Pesticide Residues on the Surface of Fruits Using Micro-Raman Spectroscopy. In D. Li, Y. Liu, & Y. Chen (Eds.), *Computer and Computing Technologies in Agriculture IV. CCTA 2010. IFIP Advances in Information and Communication Technology* (Vol. 347, pp. 427-434). Springer. doi: 10.1007/978-3-642-18369-0_50
- [30] Medina-Dzul, K., Muñoz-Rodríguez, D., Moguel-Ordoñez, Y., & Carrera-Figueiras, C. (2014). Application of mixed solvents for elution of organophosphate pesticides extracted from raw propolis by matrix solid-phase dispersion and analysis by GC-MS. *Chemical Papers*, 68, 1474-1481. doi: 10.2478/s11696-014-0600-4
- [31] Mol, H. G., Plaza-Bolaños, P., Zomer, P., de Rijk, T. C., Stolker, A. A., & Mulder, P. P. (2008). Toward a generic extraction method for simultaneous determination of pesticides, mycotoxins, plant toxins, and veterinary drugs in feed and food matrices. *Analytical Chemistry*, 80(24), 9450-9459. doi: 10.1021/ac801557f
- [32] Moros, J., Garrigues, S., & de la Guardia, M. (2010). Vibrational spectroscopy provides a green tool for multi-component analysis. *TrAC Trends in Analytical Chemistry*, 29(7), 578-591. doi: 10.1016/j.trac.2009.12.012
- [33] Moye, H. A., & Miles, C. J. (1988). Aldicarb Contamination of Groundwater. In G. W. Ware (Ed.), *Reviews of Environmental Contamination and Toxicology* (Vol. 105, pp. 99-146). Springer. doi: 10.1007/978-1-4612-3876-8_3
- [34] Nansen, C., Kolomiets, J., & Gao, X. (2008). Considerations Regarding the Use of Hyperspectral Imaging Data in Classifications of Food Products, Exemplified by Analysis of Maize Kernels. *Journal of Agricultural and Food Chemistry*, 56(9), 2933-2938. doi: 10.1021/jf073237o
- [35] Nie, S., & Emory, S. R. (1997). Probing Single Molecules and Single Nanoparticles by Surface-Enhanced Raman Scattering. *Science*, 275(5303), 1102-1106. doi: 10.1126/science.275.5303.1102
- [36] Osborne, B. G., Fearn, T., & Hindle, P. H. (1993). Near infrared calibration II. In B. G. Osborne, T. Fearn, & P. T. Hindle (Eds.), *Practical NIR Spectroscopy with Applications in Food and Beverage Analysis* (pp. 121-144). Longman Scientific & Technical.
- [37] Otto, A. J. (1991). Surface-enhanced Raman scattering of adsorbates. *Journal of Raman Spectroscopy*, 22(12), 743-752. doi: 10.1002/jrs.1250221204
- [38] Pang, S., Yang, T., & He, L. (2016). Review of surface enhanced Raman spectroscopic (SERS) detection of synthetic chemical pesticides. *TrAC Trends in Analytical Chemistry*, 85(Part A), 73-82. doi: 10.1016/j.trac.2016.06.017
- [39] Risher, J. F., Mink, F. L., & Stara, J. F. (1987). The toxicologic effects of the carbamate insecticide aldicarb in mammals: a review. *Environmental Health Perspectives*, 72, 267-281. doi: 10.1289/ehp.8772267
- [40] Roggo, Y., Chalus, P., Maurer, L., Lema-Martinez, C., Edmond, A., & Jent, N. (2007). A review of near infrared spectroscopy and chemometrics in pharmaceutical technologies. *Journal of Pharmaceutical and Biomedical Analysis*, 44(3), 683-700. doi: 10.1016/j.jpba.2007.03.023
- [41] Shende, C., Gift, A., Inscore, F., Maksymiuk, P., & Farquharson, S. (2004). Inspection of pesticide residues on food by surface-enhanced Raman spectroscopy. In G. E. Meyer, B. S. Bennedsen, Y-R. Chen, S-I Tu, A. G. Senecal (Eds.), *Monitoring Food Safety, Agriculture, and Plant Health* (Vol. 5271, pp. 28-34). International Society for Optics and Photonics.
- [42] Smith, E., & Dent, G. (2005). Introduction, Basic Theory and Principles. In E. Smith & G. Dent (Eds.), *Modern Raman Spectroscopy: A Practical Approach, First Edition* (pp.1-21). John Wiley & Sons Ltd.
- [43] Sohn, M., Himmelsbach, D. S., & Barton, F. E., II. (2004). A Comparative Study of Fourier Transform Raman and NIR Spectroscopic Methods for Assessment of Protein and Apparent Amylose in Rice. *Cereal Chemistry*, 81(4), 429-433. doi: 10.1094/CCHEM.2004.81.4.429
- [44] Štěpán, R., Tichá, J., Hájšlová, J., Kovalczuk, T., & Kocourek, V.

- (2005). Baby food production chain: Pesticide residues in fresh apples and products. *Food Additives and Contaminants*, 22(12), 1231-1242. doi: 10.1080/02652030500239623
- [45] Sun, X., & Li, H. (2016). A Review: Nanofabrication of Surface-Enhanced Raman Spectroscopy (SERS) Substrates. *Current Nanoscience*, 12(2), 175-183. doi: 10.2174/1573413711666150523001519
- [46] Tang, H., Fang, D., Li, Q., Cao, P., Geng, J., Sui, T., Wang, X., Iqbal, J., & Du, Y. (2012). Determination of Tricyclazole Content in Paddy Rice by Surface Enhanced Raman Spectroscopy. *Journal of Food Science*, 77(5), T105-T109. doi: 10.1111/j.1750-3841.2012.02665.x
- [47] U.S. Environmental Protection Agency. (n.d.). Regulation of Pesticide Residues on Food. Retrieved November 11, 2019 from <https://www.epa.gov/pesticide-tolerances>
- [48] Verma, H. N., Singh, P., & Chavan, R. M. (2014). Gold nanoparticle: synthesis and characterization. *Veterinary World*, 7(2), 72-77. doi: 10.14202/vetworld.2014.72-77
- [49] Walorczyk, S. (2007). Development of a multi-residue screening method for the determination of pesticides in cereals and dry animal feed using gas chromatography-triple quadrupole tandem mass spectrometry. *Journal of Chromatography A*, 1165(1-2), 200-212. doi: 10.1016/j.chroma.2007.07.071
- [50] Wang, Y., Lee, K., & Irudayaraj, J. (2010). Silver Nanosphere SERS Probes for Sensitive Identification of Pathogens. *The Journal of Physical Chemistry C*, 114(39), 16122-16128. doi: 10.1021/jp1015406
- [51] Watanabe, E., Miyake, S., & Yogo, Y. (2013). Review of Enzyme-Linked Immunosorbent Assays (ELISAs) for Analyses of Neonicotinoid Insecticides in Agro-environments. *Journal of Agricultural and Food Chemistry*, 61(51), 12459-12472. doi: 10.1021/jf403801h
- [52] Xu, M-L., Gao, Y., Han, X. X., & Zhao, B. (2017). Detection of Pesticide Residues in Food Using Surface-Enhanced Raman Spectroscopy: A Review. *Journal of Agricultural and Food Chemistry*, 65(32), 6719-6726. doi: 10.1021/acs.jafc.7b02504
- [53] Yuan, W., Ho, H. P., Lee, R. K. Y., & Kong, S. K. (2009). Surface-enhanced Raman scattering biosensor for DNA detection on nanoparticle island substrates. *Applied Optics*, 48(22), 4329-4337. doi: 10.1364/AO.48.004329
- [54] Zeisel, D., Deckert, V., Zenobi, R., & Vo-Dinh, T. (1998). Near-field surface-enhanced Raman spectroscopy of dye molecules adsorbed on silver island films. *Chemical Physics Letters*, 283(5-6), 381-385. doi: 10.1016/S0009-2614(97)01391-2
- [55] Zhao, L., Jiang, D., Cai, Y., Ji, X., Xie, R., & Yang, W. (2012). Tuning the size of gold nanoparticles in the citrate reduction by chloride ions. *Nanoscale*, 4(16), 5071-5076. doi: 10.1039/C2NR30957B